MIGRATE2018:208941

THERMAL ANALYSIS OF GAS CONVECTION IN POROUS MEDIA

Samy RAMDANE*, Éric CHÉNIER, Xavier NICOLAS

Laboratoire Modélisation et Simulation Multi Echelle, UMR 8208 CNRS, Université Paris-Est Marne-la-Vallée, 5 Boulevard Descartes, 77454 Marne-la-Vallée Cedex 2, FRANCE
{Samy.Ramdane,Eric.Chenier,Xavier.Nicolas}@u-pem.fr

KEY WORDS

Numerical simulation, rarefied gas flow, compressible flow, viscous dissipation, pressure work

ABSTRACT

Forced convection of a gas in porous media characterized by pores of few micrometers requires large pressure gradients. In addition to the rarefaction effects which may be significant at the solid/gas interface, we show that it may be necessary to account for the pressure work and the viscous dissipation in the energy equation to get the right temperature field induced by the fluid flow.

Introduction

In recent years, there has been a great interest in fluid flows through geological or artificial micro-porous media, for example to improve the heat transfer in micro channels [4], to separate small molecules from a gaseous mixture [2] or to extract gas from shale strata using large pressure gradients [1]. In this work, we focus on the thermal effects produced by a gas flowing between a periodic network of solid obstacles separated by a few micrometers, under large pressure gradients.

Geometry and mathematical model

We are interested in a gas flowing through a 3D network of parallel bars of rectangular section (8 μm×4 μm) spaced regularly by 8 and 4 μm in x- and y-directions. Assuming that their length is large enough with respect to their section, a 2D geometrical model may be adopted (Fig. 1). Despite the geometrical periodicity of the problem, this property cannot be imposed in the flow direction since the density changes when the pressure decreases.

We then consider a set of 10 adjacent Representative Elementary Volumes in the x-direction, with symmetry conditions at $y=0$ and $y=L_1/2$. The inlet and outlet pressures (p_{in} and p_{out}) are imposed as well as the inlet temperature (T_{in}). The velocity and temperature fields are assumed fully developed at the outlet. The velocity $\boldsymbol{v} = u\boldsymbol{e_x} + v\boldsymbol{e_y}$, the pressure p and temperature T_f in the fluid phase are solutions of the Navier-Stokes and energy equations written with the Newtonian viscosity model and the Stokes assumption for the bulk viscosity. Because the pressure remains moderate, the ideal gas law is considered. The dynamic viscosity μ, the fluid k_f and solid k_s thermal conductivities and the specific heat c_p are assumed constant. The fluid steady governing equations write :

$$\forall\, \boldsymbol{x} \in \Omega_f, \begin{cases} \boldsymbol{\nabla}.(\rho \boldsymbol{v}) = 0 \\ \boldsymbol{\nabla}.(\rho \boldsymbol{v} \otimes \boldsymbol{v}) + \boldsymbol{\nabla} p - \boldsymbol{\nabla}.\bar{\bar{\tau}} = 0 \\ c_p \boldsymbol{\nabla}.\left(\rho \boldsymbol{v} T_f\right) - \boldsymbol{v}.\boldsymbol{\nabla} p - \bar{\bar{\tau}} : \bar{\bar{d}} - \boldsymbol{\nabla}.\left(k_f \boldsymbol{\nabla} T_f\right) = 0 \\ p - \rho r T_f = 0 \end{cases} \quad (1)$$

with $\bar{\bar{\tau}}$ the viscous stress tensor, $\bar{\bar{d}}$ the strain rate tensor, r the specific gas constant and Ω_f the fluid domain. In the solid phase, the temperature is solution of the steady conduction equation:

$$\forall\, \boldsymbol{x} \in \Omega_s, \boldsymbol{\nabla}.(k_s \boldsymbol{\nabla} T_s) = 0 \quad (2)$$

with T_s the solid temperature and Ω_s the solid domain. Since rarefaction effects are assumed to take place at the solid/fluid interface Ω_{fs}, jump conditions must be accounted for:

$$\forall\, \boldsymbol{x} \in \Omega_{fs}, \begin{cases} \boldsymbol{v} = -\xi_v \lambda \left(\bar{\bar{I}} - \boldsymbol{n_{fs}} \otimes \boldsymbol{n_{fs}}\right).\left(2\bar{\bar{d}}.\boldsymbol{n_{fs}}\right) \\ T_s = T_f + \xi_T \lambda \frac{\partial T_f}{\partial \boldsymbol{n_{fs}}} \\ k_s \frac{\partial T_s}{\partial \boldsymbol{n_{fs}}} = k_f \frac{\partial T_f}{\partial \boldsymbol{n_{fs}}} + 2\mu \boldsymbol{v}.\left(\bar{\bar{d}}.\boldsymbol{n_{fs}}\right) \end{cases} \quad (3)$$

with $\boldsymbol{\xi_v}$ and $\boldsymbol{\xi_T}$ the dynamic and thermal accommodation parameters, $\lambda = \frac{\mu}{p}\sqrt{(\pi r T_f)/2)}$ the mean free path of gas molecules and $\boldsymbol{n_{fs}}$ the unit normal vector pointing outside the fluid domain. The physical properties are those of nitrogen (r=296 J/(kg K), μ=1.6588 10^{-5} Pa s, c_p=1032.48 J/(kg K), k_f=2.4712 10^{-2} W/(m K)) and aluminum (k_s=240 W/(m K)).

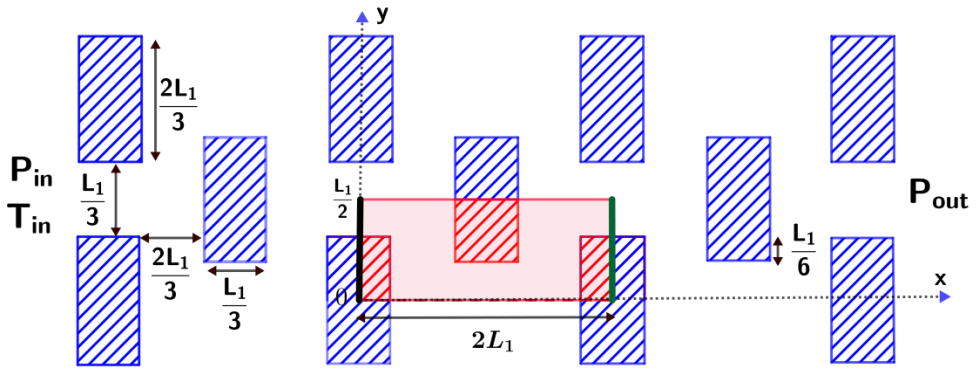

Figure 1: Characteristic dimensions in the section plane (L_1=12µm). The red domain stands for one Representative Elementary Volume

Numerical methods

An unstructured collocated finite volume scheme [3] is used to solve the steady Navier-Stokes and energy equations with the ideal gas law (Eqs. 1 and 2), the aforementioned boundary conditions and the solid/fluid interface relations (Eq. 3). The coupled discrete equations are solved simultaneously with a Newton-Raphson algorithm.

The mesh is based on a triangular tessellation with coarse elements of size $0.5L_1/80$ in the core flow and fine elements with edges 8 times smaller close to the fluid/solid interface. A buffer zone of size $0.1L_1$ connects the 2 regions. Reducing the grid size by 2 changes the maxima and minima of the velocity and temperature by less than 1%. We conclude that the solutions are enough accurate with the

first described mesh. Notice that very expensive unsteady simulations have also been carried out to confirm the steadiness of the solutions.

Results

As indicated previously, simulations are carried out over 10 REV of height 6 µm, covering a total length of 240 µm for a 1,6 bar pressure variation between the inlet and outlet and a mean pressure of 2 bar. The Knudsen number based on the smallest cross-section length, $Kn=3\lambda/L_1$, ranges from $5{,}5.10^{-3}$ to $1{,}28.10^{-2}$.

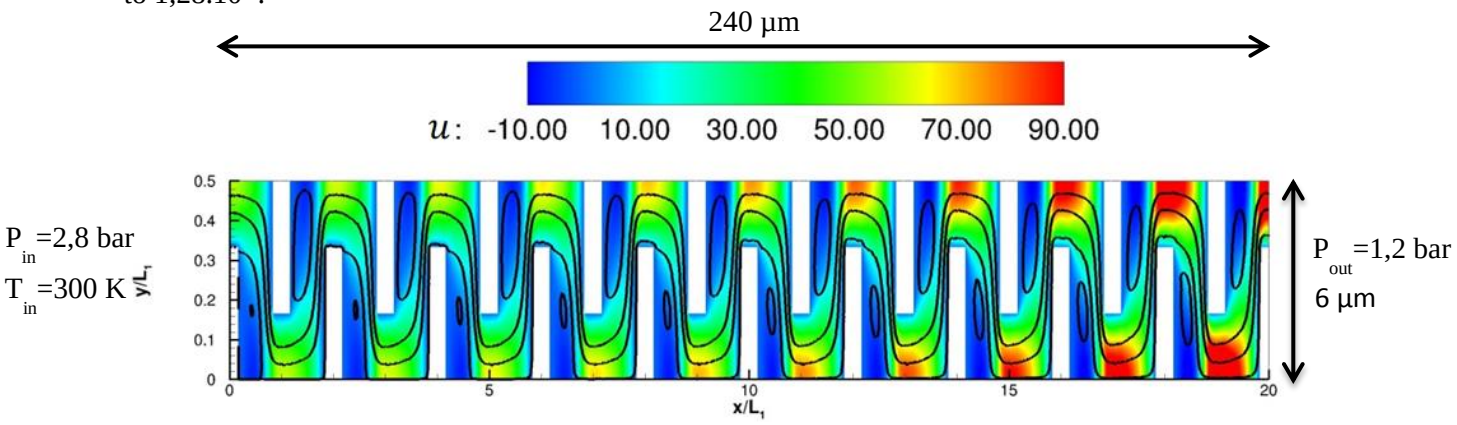

Figure 2 : Horizontal component of the velocity (m/s) and stream lines in black

Fig. 2 presents the horizontal component of the velocity and some stream lines. The decrease in the pressure downstream creates a drop in the gas density and, considering the mass flow rate conservation, an increase in the velocity. The Reynolds number based on the mass flow rate is about 28, what explains the steady recirculations occurring behind the solid obstacles.

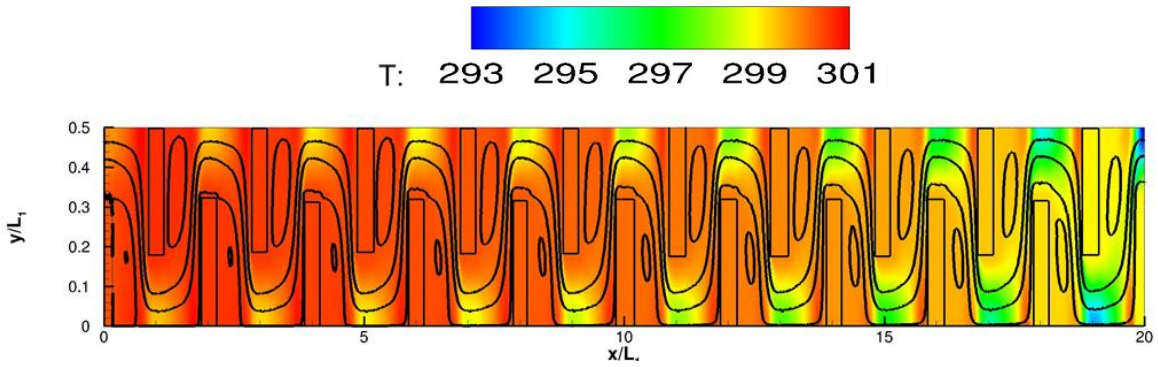

Figure 3 : Temperature field (K) in the fluid and solid domains. Stream lines are indicated in black

Fig. 3 shows the temperature field, both in the solid and in the fluid. On the whole, the average temperature decreases in the flow direction. The maximum temperature difference in the whole field on Fig. 3 reaches about 8 K. Whereas the viscous dissipation heats up the gas, the pressure work contribution is more complex since it depends on the direction of the pressure gradient. Generally, the fluid flows from high to low pressure regions by extracting some amount of thermal energy. However upstream solid obstacles, the pressure gradient reverses what produces a heat source in the fluid. The analysis of Fig. 3 indicates that the cooling by the pressure work dominates the viscous dissipation. Due to the very high ratio between the solid and fluid conductivities, the temperature in the solid domain appears completely uniform.

To better understand the temperature variations, the 7th REV is studied more thoroughly. Fig. 4 presents the difference between the local temperature and the average temperature in the fluid phase only. The thick black lines split the physical domain into regions colder or warmer than the average value. This figure first indicates that the solid obstacles are hotter than the fluid is. This is mainly due to the viscous dissipation which occurs close to the fluid/solid interface but also to the pressure work because the pressure gradient reverses just in front of the obstacles and close to the symmetry boundaries (see the red spot in Fig. 4). The colder regions are located right above or below the solid blocs where the velocity and gradient vectors are collinear but with opposite directions.

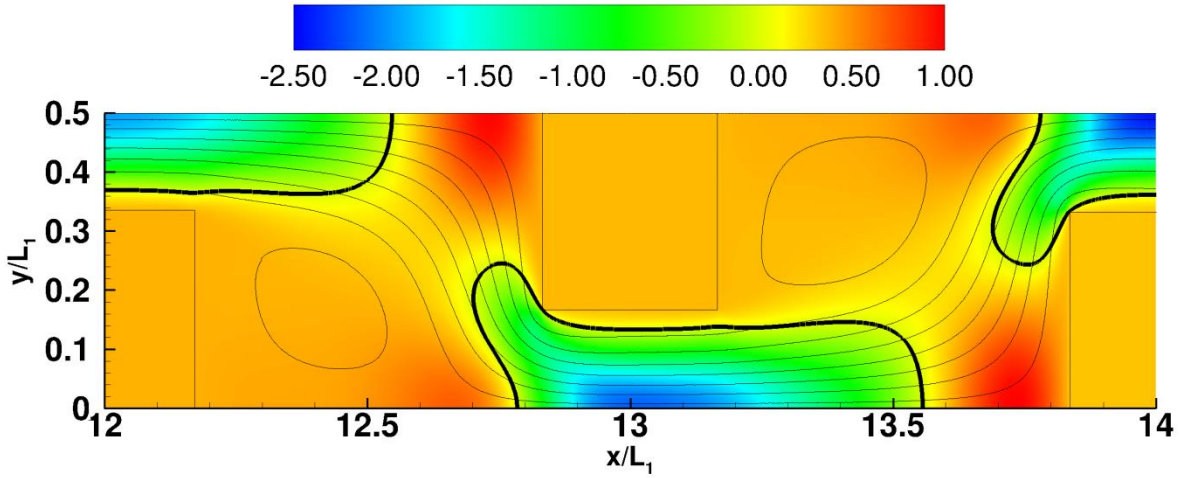

Figure 4 : Difference between the local and mean fluid temperature, for the 7th REV. Stream lines are drawn with thin black lines. The thick lines indicate the places where the local temperature is equal to the average fluid temperature.

Conclusion

In this short paper, we have briefly illustrated and analyzed the thermal effects created by a gas flow submitted to large pressure gradients in porous media made of micrometric pores. The pressure work and viscous dissipation effects have been particularly discussed. Their thermal effects are not negligible.

References

[1] H. Darabi. A. Ettehad. F. Javadpour., & K. Sepehrnoori (2012). Gas flow in ultra-tight shale strata. J. Fluid Mech, vol. 710, pp. 641-658.

[2] S. Nakaye. H. Sugimoto N.K. Gupta Y.B., & Gianchandani (2015). Thermally enhanced membrane gas separation. European Journal of Mechanics, vol. 49, pp. 36-49.

[3] O. Touazi, E. Chénier., & R. Eymard. (2008). Simulation of natural convection with the collocated clustered finite volume scheme, Computers & Fluids, vol. 37, pp. 1138-1147.

[4] K. Wang K. Vafai., & D. Wang. (2015). Analytical characterization of gaseous slip flow and heat transport through a parallel-plate microchannel with a centered porous substrate. International Journal of Numerical Methods for Heat and Fluid Flow, vol. 26, pp. 854-878.